Light particle emission in $^{35}Cl + ^{24}Mg$ fusion reactions at high excitation energy and angular momentum

D. Mahboub,* C. Beck, B. Djerroud, R. M. Freeman, F. Haas, R. Nouicer,† M. Rousseau, P. Papka, and A. Sànchez i Zafra
Institut de Recherches Subatomiques, UMR7500, CNRS-IN2P3 et Université Louis Pasteur, Boîte Postale 28, F-67037 Strasbourg CEDEX 2, France

Sl. Cavallaro, E. De Filippo, G. Lanzanò, A. Pagano, and M. Sperduto
Istituto Nazionale di Fisica Nucleare and Dipartimento di Fisica, I-95129 Catania, Italy

E. Berthoumieux, R. Dayras, R. Legrain,‡ and E. Pollacco
DAPNIA/SPhN CEA-Saclay, F-91191 Gif-sur-Yvette, France

A. Hachem
Faculté des Sciences, Université de Nice-Sophia-Antipolis, F-06034 Nice, France
(Received 28 August 2003; published 29 March 2004)

In-plane and out-of-plane correlations of light charged particles and neutrons emitted in the ^{35}Cl (260 MeV) + ^{24}Mg complete fusion reaction have been measured to investigate deformation and angular momentum effects upon the decay of ^{59}Cu compound nucleus. An array of 21 BaF_2 crystals has been used to identify the light charged particles ($Z \leqslant 4$) and neutrons emitted in coincidence with heavy fragments ($Z \geqslant 5$) detected in six ionization chamber telescopes. Coincident energy spectra and angular distributions of neutrons, protons, and α-particles have been described by the statistical-model calculations with nuclear level densities tuned to take account of deformation effects in the emitters. This spin-dependent approach suggests the onset of large nuclear deformation in ^{59}Cu at high spin. This conclusion is consistent with the recent observation of a superdeformed band in the ^{59}Cu nucleus.

DOI: 10.1103/PhysRevC.69.034616 PACS number(s): 25.70.Gh, 25.70.Jj, 24.60.Dr, 27.50.+e

I. INTRODUCTION

Over the past few years, deep-inelastic (DI) orbiting collision, fusion-fission (FF), and fusion-evaporation (FE) processes between light heavy ions have been extensively studied [1–3] in order to investigate the macroscopic properties of highly excited and deformed dinuclei. Some of the characteristic properties of hot nuclei at high spin have been well explained in the framework of existing FF models [1,4] indicating that DI process is not the dominant mechanism in the $45 \leqslant A_{CN} \leqslant 60$ light-mass region. In this context the ^{35}Cl (280 MeV) + ^{24}Mg reaction has been studied in great detail [5–11]. It has been shown that after complete fusion (CF) asymmetrical fission [6,8] occurs at a significant level for the ^{59}Cu compound nucleus (CN) according to what has been observed previously for neighboring nuclei [1,4]. However, the possible contribution of a long-lived DI process could not be ruled out [6]. At high excitation energy and angular momentum a rich variety of nuclear shapes can be encountered. For example, variations in the nuclear deformation should be reflected in particle emission through modification of the emission barriers and nuclear level densities. A number of studies have used the light charged particle (LCP) emission to probe the individual reaction mechanisms in the light-mass region under consideration [12–37]. In particular, a statistical-model analysis of α-particle spectra shapes in coincidence with the evaporation residues (ER) from ^{59}Cu produced in the $^{32}S + ^{27}Al$ reaction suggests strong angular momentum induced deformations, larger than those predicted by rotating liquid-drop model (RLDM) calculations [12–15]. Furthermore, superdeformed (SD) rotational bands have been found in various mass regions ($A = 40$, 60, 80, 130, 150, and 190) and, very recently, one SD band has also been discovered in the ^{59}Cu nucleus [38–41] in agreement with the predictions of either Skyrme-Hartree-Fock and Strutinsky-Woods-Saxon calculations [42] or relativistic mean-field theories [43].

As an attempt to understand why these systems undergo a FF process, we propose to investigate their shapes at high excitation energy and angular momentum. In this paper, experimental results are presented on light particle (LP) emission (both LCP and neutron emission are considered) following the FE of the ^{59}Cu CN formed in the ^{35}Cl (260 MeV) + ^{24}Mg reaction. The analysis is intended to provide insight into the deformation of this CN. Inclusive experiments have already been dedicated to the α-particle evaporation from the ^{59}Cu CN formed by the $^{32}S + ^{27}Al$ entrance channel [12–15] but they were largely limited to inclusive α-particle energy spectra. We shall focus here on exclusive LP angular correlations for the FE process. The $^{35}Cl + ^{24}Mg$ reaction has been studied extensively using inclusive data [5,6] and fragment-fragment angular correlations data [7,8] measured at some-

*Present address: University of Surrey, Guildford GU2 7XH, United Kingdom.
†Present address: Brookhaven National Laboratory, Upton.
‡Deceased.

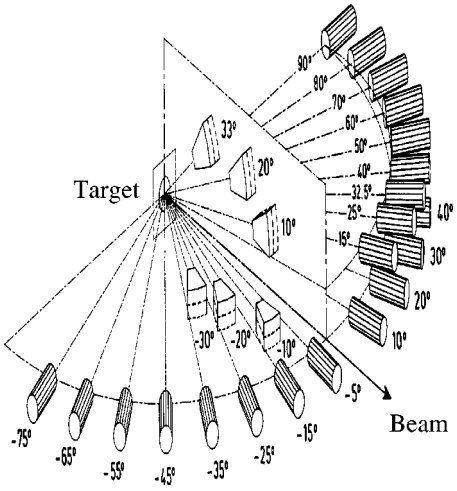

FIG. 1. Experimental setup of the LP-fragment correlation measurements for the ^{35}Cl+^{24}Mg reaction at $E_{lab}(^{35}\mathrm{Cl})=260$ MeV.

what higher incident energies $[E_{lab}(^{35}\mathrm{Cl})\approx 280$ MeV$]$. The results have shown that the FF process is also an open channel to produce the binary reaction products. Preliminary LP results of the present work have already been reported elsewhere [9]. Exclusive measurements of LCP from both FF and DI processes [10] will be discussed in a forthcoming publication.

The paper is organized in the following way. The experimental setup and LP discrimination techniques are described briefly in the following section. The experimental results are presented in Sec. III. Section IV contains the description of the theoretical framework for the statistical model using a Monte Carlo version of the CASCADE Hauser-Feshbach evaporation code [12,13,44]. This is followed by a detailed comparison of its predictions with the experimental results. Concluding remarks are presented in Sec. V.

II. EXPERIMENTAL PROCEDURES

The experiment was performed at the Saclay Post-Accelerator Tandem Facility. The 260 MeV ^{35}Cl pulsed beam was incident on a 250 μg/cm^2 thick, self-supporting, 99.9% enriched ^{24}Mg target mounted in the 2 m diameter scattering chamber "chambre 2000." Carbon and oxygen contaminants in the target were each estimated to be less than 10 μg/cm^2 thick, using a 2 MeV α-beam backscattering technique [6]. The time structure of the pulsed beam had a period of 74 ns and was used in the time-of-flight (TOF) measurement. The experimental setup, displayed in Fig. 1, consisted of both heavy-ion telescopes and LP detectors.

The ERs and other reaction products were detected in six small ionization chamber (IC) telescopes located in two perpendicular planes, the intersection of which was along the beam axis (see Fig. 1). Three ICs were located in the horizontal plane, on the same side of the beam at $\theta_{lab}=-10°$, $-20°$, and $-30°$. The three remaining ICs were located in the vertical plane $\theta_{lab}=10°, 20°$, and 33°, defining an out-of-plane configuration for the LP detectors. As shown in Fig. 1, the distance of these telescopes from the target ranged from

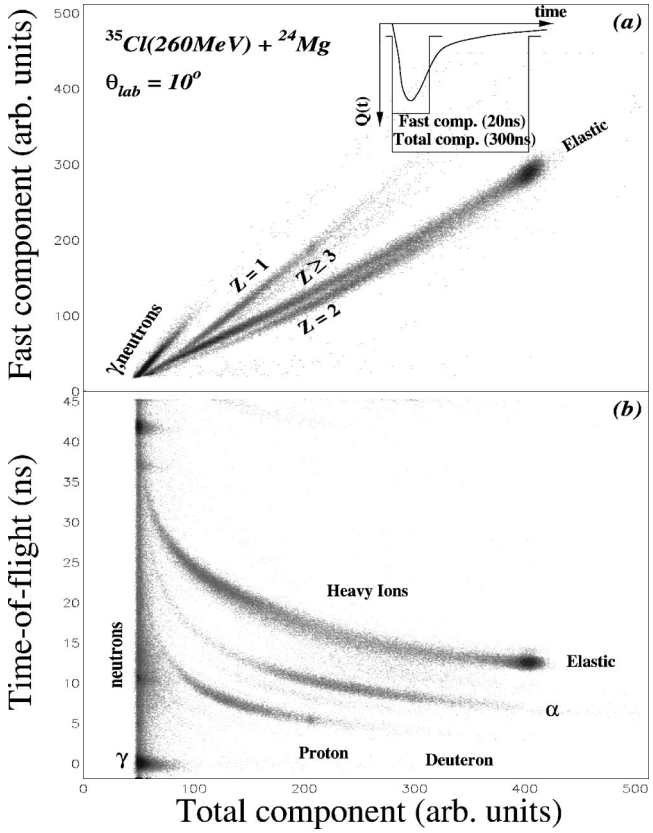

FIG. 2. Bidimensional LP spectra measured in the ^{35}Cl+^{24}Mg reaction at the indicated angle. (a) Fast component vs total component scatter plot. (b) TOF vs total component scatter plot. The inset shows the positions of the gates relative to the anode signal in order to extract the fast and total components of the BaF_2 signal.

$d=13.0$ to $d=42.0$ cm, and the solid angles varied from $\Delta\Omega=0.45$ msr at the most forward angles to $\Delta\Omega=4.79$ msr at the backward angles according to the expected counting rate. Each of the ICs was filled with CF_4 gas at a pressure of 52 Torr and followed by a 500 μm thick Si(SB) detector. The energy calibration of the telescopes was carried out using elastically scattered ^{35}Cl projectiles from 250 μg/cm^2 thick Au and 100 μg/cm^2 thick C targets and from the ^{24}Mg target, combined with measurements with α sources and a precision pulse generator. On an event-by-event basis, corrections were applied for energy loss in the target and in the entrance Mylar window foils on the ICs and for the pulse height defect in the Si detectors. To correct for the carbon contamination, measurements were also made at the same detector angles and with comparable beam conditions using the 100 μg/cm^2 thick, self-supporting, carbon foil as a target. Further details of the experimental procedures can be found elsewhere [3,6,8] in the description of similar measurements.

The LCPs and neutrons were identified with an array of 21 hexagonal BaF_2 crystals [45] using the pulse-shape discrimination technique in conjunction with TOF measurements. Each crystal was 10 cm thick and 31.5 mm width, stopping protons up to 200 MeV. The front faces were covered with thin aluminized Mylar, 2 μm thick. Most of the 21 BaF_2 crystals were located at a distance of $\approx$52 cm from

the target in the horizontal plane (see Fig. 1) between $\theta_{lab} = -75°$ and $\theta_{lab} = +90°$ in order to permit both the in-plane and out-of-plane angular correlation measurements. Asymmetry corrections were applied for the eight scintillators which were not located precisely in the horizontal plane between $\theta_{lab} = +15°$ and $\theta_{lab} = +80°$. Typical particle identification spectra are shown in Fig. 2 in which (a) the charge and (b) the mass discrimination are easily achieved. A perfect isotopic separation of all LCPs up to $Z=3$ and $A=7$ was possible when combining the TOF and the pulse-shape discrimination techniques (cf. Fig. 2). Although its efficiency has an energy dependence [46], neutron detection [10] was also achieved, however with a rather low efficiency of about 8% [46].

The BaF_2 crystals were calibrated using TOF technique with the time reference given by the peak position of the prompt γ rays. LCP and neutron velocities V and energies E were deduced from the total charge output induced by the scintillating light signal "l" with the simplified nonlinear relations proposed by Lanzanò *et al.* [45]:

$$E(\mathrm{MeV}) = al^{\beta} + b, \tag{1}$$

$$\text{and} \quad V(\mathrm{cm/ns}) = \alpha\sqrt{al^{\beta} + b}, \tag{2}$$

where for each particle species the parameter β is known to be a universal constant [45]. The β values were thus taken to be the mean values obtained from the fits performed for all the scintillators: $\beta=0.91$ for protons and 0.83 for α particles, respectively (see Ref. [10] for details). Due to the fact that reasonable particle discrimination is very difficult to achieve at very low energy for both representations (fast, total; TOF, total), energy thresholds of about 2.0 MeV for protons and 5.0 MeV for α particles were imposed.

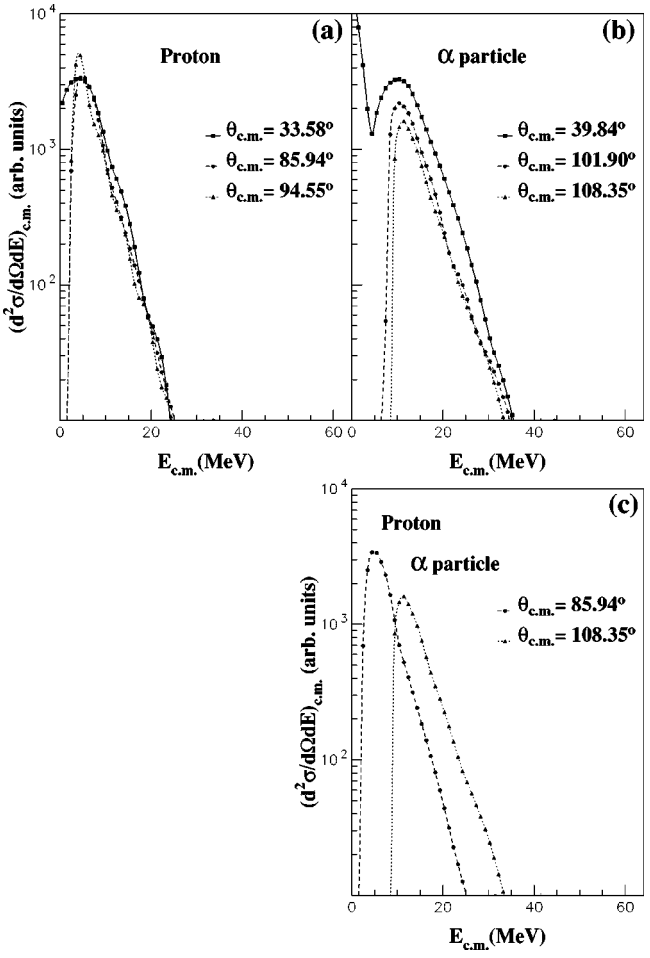

FIG. 3. Inclusive proton (a) and α-particle (b) kinetic energy spectra measured in the center-of-mass system for the $^{35}Cl+^{24}Mg$ reaction at the indicated c.m. angles. (c) Comparison between proton and α-particle energy spectra.

III. EXPERIMENTAL RESULTS

A. Inclusive measurements

Typical inclusive LCP kinetic energy spectra in the center-of-mass (c.m.) frame are presented in Fig. 3 at the indicated c.m. angles. The energy spectra have a Maxwellian form with an exponential falloff at high energy. A comparison [see Fig. 3(c)] between the α-particle and proton energy spectra shows that they have the same trend and slope; they differ only in the positions of their maxima due to higher emission barrier for α particles. This is consistent with a statistical deexcitation process arising from a thermalized source. We assume that the exponential slope at high energy, which is independent of LCP angle detection, can be considered as a nuclear thermometer. Thus the LCP arises from an evaporation process of a decaying nucleus which has been heated to a relatively high temperature ($4\ \mathrm{MeV} \leqslant T \leqslant 5\ \mathrm{MeV}$) as will be discussed in the following. Some knoblike distortions, due to the decay from fragments in binary decay processes, appear on the high-energy slopes, and LCP preequilibrium contributions are found to be negligible in agreement with the inclusive data [5,6] and the fragment-fragment coincidence data [7,8] available for the $^{35}Cl+^{24}Mg$ reaction. The incomplete fusion (ICF) cross section has been measured to be less than 60 mb at $E_{lab} = 280$ MeV [6] and therefore represents only a very small (3%) portion of the total reaction cross section **(**estimated to be $\approx$1800 mb according to the optical model (OM) analysis of the measured elastic scattering [6]**)**. This conclusion is consistent with evidence of ICF and preequilibrium emission which was found only at higher incident energies [22,47] ($E_{lab} = 10-15$ MeV/nucleon).

B. Exclusive measurements

Typical proton and α-particle coincident energy spectra in the laboratory frame are shown in Fig. 4 for the ERs detected at $\theta_{lab} = -10°$ with $18 \leqslant Z \leqslant 24$ at the indicated laboratory angles. In order to know more about the source of the LCP, Galilean-invariant differential cross sections $(d^2\sigma/d\Omega dE)p^{-1}c^{-1}$ plotted in the $V_{\parallel}-V_{\perp}$ map are displayed in Fig. 5 for the protons and α particles in coincidence with ERs having $Z=20, 22$, and 23, respectively. $V_{\parallel}$ and $V_{\perp}$ denote the laboratory velocity components parallel and perpendicular to the beam, respectively. The mean values of the ER

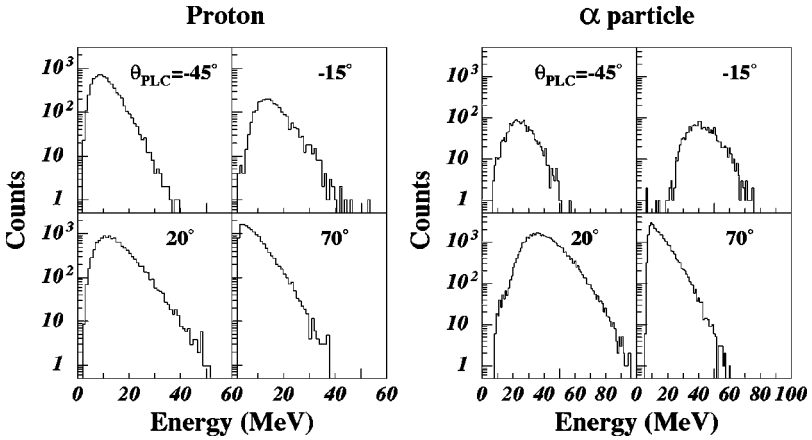

FIG. 4. Exclusive proton and α-particle kinetic energy spectra measured in coincidence with ERs in the laboratory system for the $^{35}Cl+^{24}Mg$ reaction at the indicated laboratory angles. The ERs ($18 \leqslant Z \leqslant 24$) were detected in-plane by the IC located at $\theta_{lab}=-10°$.

velocities are represented by a thick arrow. The circles are defined to visualize the maxima of production; their centers correspond to the mean values and directions of the velocities of the emitters and are represented by thin arrows. It can be seen that the largest part of the yield is concentrated at the opposite side of the emitter with respect to the beam axis due to the momentum conservation law. The most important result which can be drawn from these plots is that all the spectra can be understood by assuming a single source; consistent with the CN origin. This leads to the conclusion that no evidence of preequilibrium emission either from the target or from the projectile has been observed. Components of preequilibrium emission from other sources would have imposed repulsion barriers smaller than those indicated in Fig. 5. Other smaller radius circles centered in either the projectile or target velocity are needed to account for the yield of the LCPs. These facts justify a confrontation of the data with a statistical-model code which will be presented in the following section.

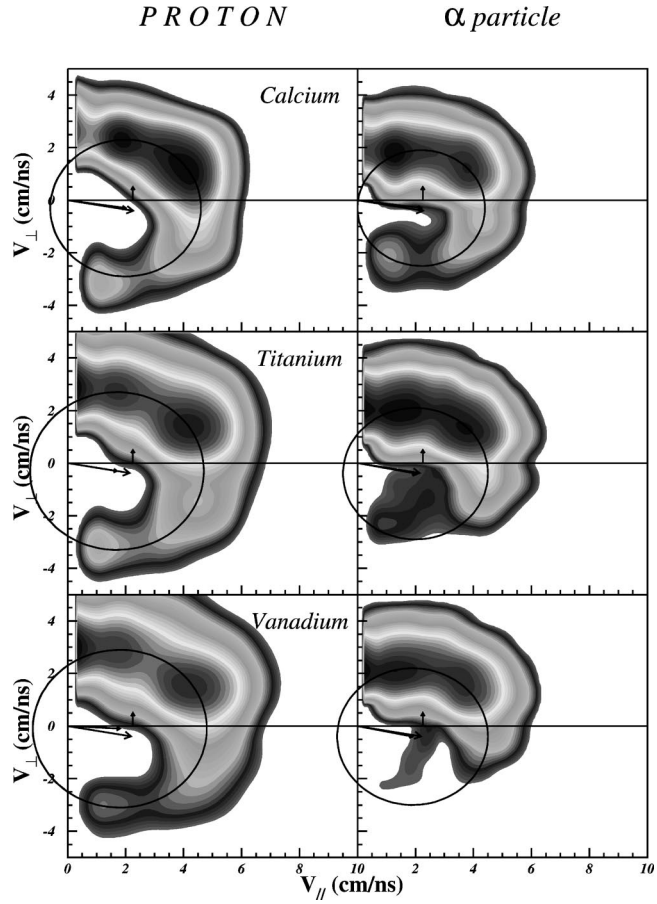

FIG. 5. Exclusive proton and α-particle Galilean-invariant cross sections measured in coincidence with Ca, Ti, and V ERs for the $^{35}Cl+^{24}Mg$ reaction. Galilean-invariant cross sections are plotted as a function of the perpendicular and parallel velocities with respect to the beam axis. The ERs were detected in-plane at $\theta_{lab}=-10°$. Thick arrows indicate the mean velocity of the ER and the thin one indicates the center of the circle.

In-plane and out-of-plane angular correlations are presented in Figs. 6 and 7 for protons and α particles in coincidence with all ERs detected at the indicated angles. The in-plane correlations displayed in Fig. 6 are peaked at the opposite side from the ER detectors with respect to the beam. These correlations are found to be much flatter for the protons than for α particles. By neglecting the Coulomb barrier differences and by assuming the same emission temperature, the α emission velocities are half those of the protons, which constrains the α particles to a much narrower solid angle cone (forward peaked) than the protons. The out-of-plane angular correlations displayed in Fig. 7 have a behavior in

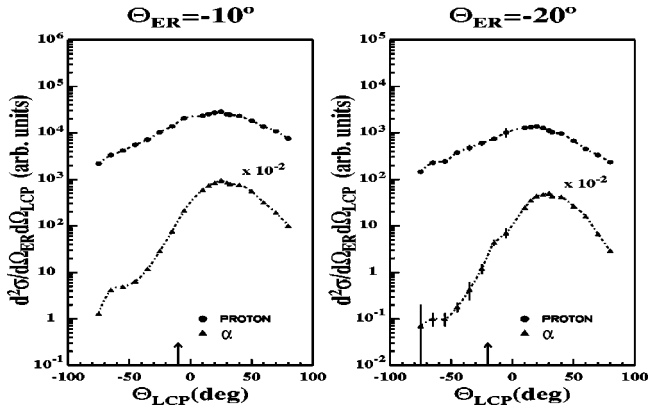

FIG. 6. In-plane angular correlations of protons and α particles in coincidence with ERs in the laboratory system for the $^{35}Cl+^{24}Mg$ reaction. The ERs were detected in-plane at $\theta_{ER}=-10°$ and $\theta_{ER}=-20°$. The dashed lines are a guide to the eye.

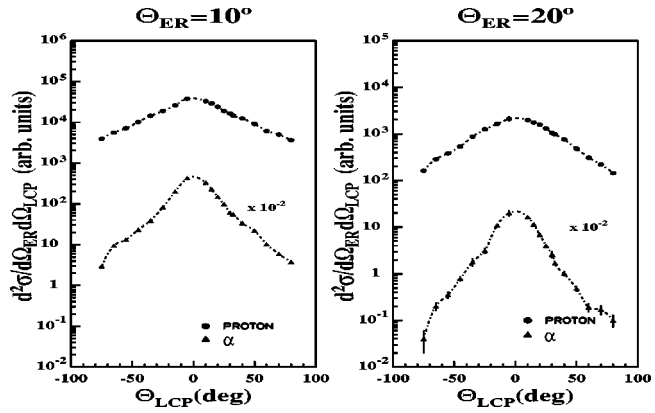

FIG. 7. Same as Fig. 6 for out-of-plane angular correlations. The ERs were detected in the vertical plane (see Fig. 1) at $\theta_{ER}=+10°$ and $\theta_{ER}=+20°$.

$\exp[-a\sin^2(\theta_{lab})]$, with two possible distinct components visible in the α-particle angular correlations with a broadening at backward angles. This effect may be due to the fact that the α particles can be emitted either at the beginning or at the end of the decay chain when the angular momentum is smaller. The proton cannot remove as much angular momentum as the α particles. This is the main reason why this effect is much less significant in the proton angular correlation.

By using a simple Weisskopf approach to predict the energy shape of LP spectra, i.e., LCP and neutrons evaporated from an equilibrated and fully thermalized source, the probability of emitting a LCP and/or a neutron with energy ε is given by the following expression [10,59,60]:

$$P_x(\varepsilon) \propto \begin{cases} 0 & \text{for} \quad \varepsilon < B_x \\ \dfrac{\varepsilon - B_x}{T'^2}\exp\left(-\dfrac{\varepsilon - B_x}{T'}\right) & \text{for} \quad \varepsilon > B_x, \end{cases} \tag{3}$$

where B_x is the emission barrier of the charged particle x. Its value is equal to zero in the case of neutron emission. The slope parameter T', or apparent temperature, can be directly related to the nuclear temperature parameter T (NTP) of the emitting source. The NTP can be deduced from the excitation energy E^* using the Fermi-gas model formula $E^*=aT^2$, where a is the well known level-density parameter. Despite its simplicity, formula (3) can explain the observed Maxwellian shape of the measured energy spectra as shown in Fig. 8. We have attempted to extract the NTP as well as the emission barrier by fitting the experimental energy spectra of the LP in the frame of the parent nucleus. Table I gives the results of the NTPs for each emitter. Knowing that the detected LP can be emitted from any stage of the evaporation cascade, this approximation may appear to be too simplistic. However it has been checked that the stage of emission has a strong effect on the emission barrier only, and not on the slope parameter which is of interest here.

Figure 8 shows the result of the fitting procedure applied to the energy spectra measured in the emitter reference frame (as deduced from the detected ER). The Maxwellian shape was used for neutrons, protons, and α particles and is shown as a function of the detection angle. Since there is essentially no angular dependence of the slope parameter for each LP (see Fig. 9), a mean value of the apparent temperature has been deduced for each ER.

A correction of the NTP, due to the rotational motion, needs to be introduced [54] in order to make the values extracted for the protons or the α particles consistent. This correction, which takes into account the average energy carried away by the LP, as well as their separation energy from the composite system and the rotational energy [54], is given by the following approximate formula [10]:

$$T = \left(1 - \frac{5m}{2M}\right)T', \tag{4}$$

where T' is the apparent temperature extracted from the slope parameter, and m and M are the masses of the LP and ER, respectively.

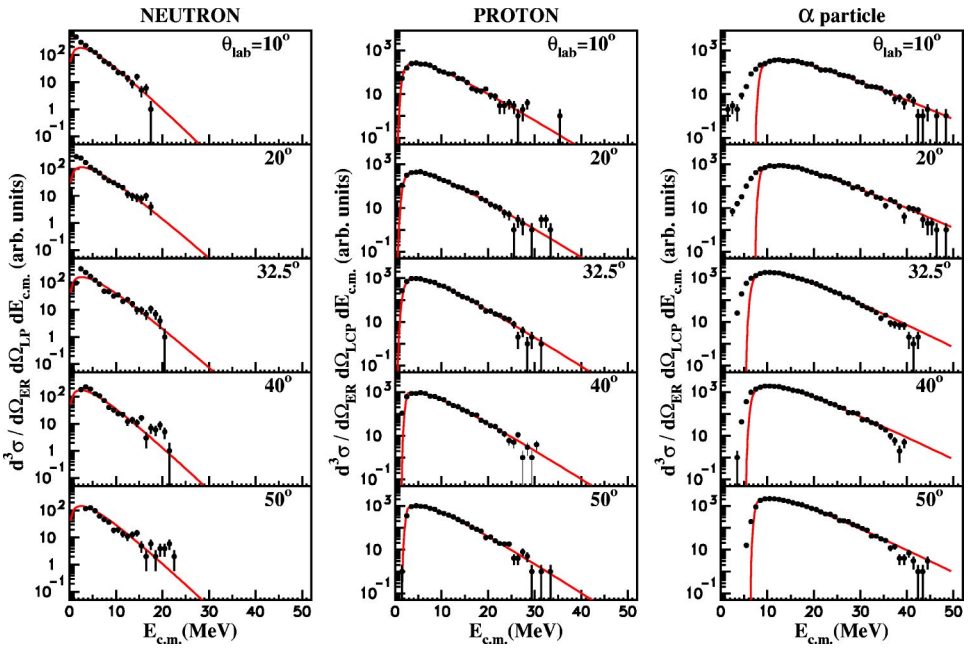

FIG. 8. (Color online) Kinetic energy spectra of neutrons, protons, and α particles detected at the indicated angles in coincidence with Ti residues, plotted in the frame of the emitting source for the ^{35}Cl+^{24}Mg reaction. The Ti residues were detected in-plane at $\theta_{ER}=-10°$. The solid lines are Maxwellian fits which are described in the text.

TABLE I. Apparent temperature parameter T' and nuclear temperature parameter T of the indicated ERs as extracted from the LCP and neutron energy spectra in the source reference frame (see text). The quoted error bars are only statistical and do not include a systematic uncertainty of ≈10%.

LP	Emitting fragment	Detected fragment	T' (MeV)	T (MeV)
Neutron	22	22	2.56±0.50	2.40±0.50
	24	24	3.61±0.50	3.44±0.50
Proton	19	18	2.23±0.02	2.09±0.02
	20	19	2.40±0.02	2.25±0.02
	21	20	2.51±0.02	2.37±0.02
	22	21	2.81±0.01	2.66±0.01
	23	22	3.11±0.01	2.95±0.01
	24	23	3.40±0.01	3.23±0.01
	25	24	3.82±0.03	3.64±0.03
α	20	18	3.51±0.03	2.67±0.03
	21	19	3.49±0.02	2.69±0.02
	22	20	3.64±0.02	2.86±0.02
	23	21	3.68±0.01	2.93±0.01
	24	22	4.08±0.01	3.28±0.01
	25	23	4.80±0.02	3.90±0.02
	26	24	5.69±0.05	4.68±0.05

A phenomenological approach has been used to determine the NTP from the excitation energy of the fragments in a cascade leading to the ER of interest. Using the Fermi-gas model formula we can deduce the NTP by using two different and extreme values of the level-density parameter: $a=A/12$ or $A/8$. The latter value is the standard one which is commonly used in statistical-model calculations [1,4] performed in the mass region considered, however a decrease at higher excitation energies of the value of the level-density parameter up to $a=A/12$ has also been found adequate in higher-mass systems for some cases [47–53]. The mean excitation energy removed by the LP, referring to our recent systematic results, [3,8] has been taken to be approximately 16 MeV and 22 MeV for proton and α-particle, respectively. The remaining excitation energy can be calculated for the daughter nucleus as shown in Table II. The values of the NTP thus calculated are compared to the values deduced from the fits in Fig. 10. The full line has been calculated with $a=A/8$ and the dashed line with $a=A/12$. Within the error bars (including systematic uncertainties of ≈10%) the experimental data are satisfactorily reproduced with $a=A/8$, a value which appears to be consistent with previous work [20,55,57]. This value will be used as an input for the statistical-model calculations described in the following section. We note that for the fragments obtained from two cascades a weighted mean value has been calculated favoring the cascade which contains more α particles.

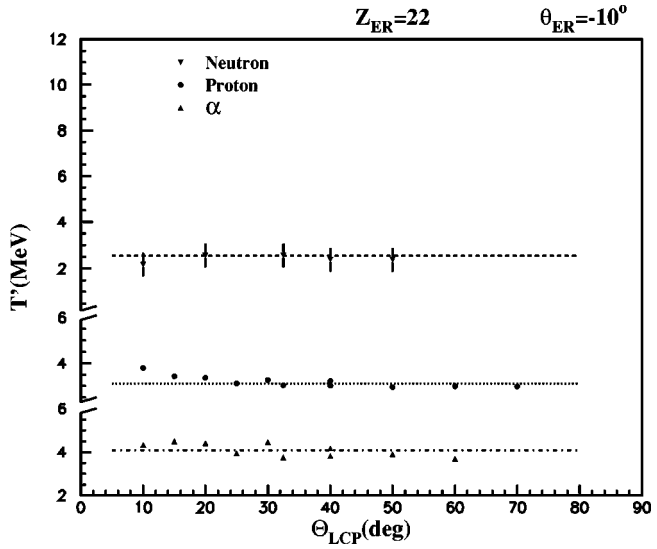

FIG. 9. Angular dependence of the apparent temperature extracted from the kinetic energy spectra of neutrons, protons, and α particles detected in coincidence with Ti residues at $\theta_{ER}=-10°$.

TABLE II. Nuclear temperature parameter T of the indicated ERs estimated with the two indicated values of the level-density parameter.

Nucleus (Z,A)	Cascade	E^*(MeV)	$T(A/8)$ (MeV)	$T(A/12)$ (MeV)
29–59		119.3	4.02	4.93
28–58	$1p$	102.9	3.77	4.61
27–57	$2p$	86.5	3.48	4.27
26–54	$1\alpha,1p$	80.8	3.46	4.24
25–53	$1\alpha,2p$	64.4	3.12	3.82
25–51	2α	75.1	3.43	3.20
24–51	$1\alpha,3p,1n$	31.6	2.23	2.73
24–50	$2\alpha,1p$	58.7	3.07	3.75
23–49	$1\alpha,4p,2n$	−1.2		
23–49	$2\alpha,2p$	42.3	2.63	3.22
23–47	3α	53.0	3.00	3.68
22–47	$1\alpha,5p,3n$	−34.0		
22–47	$2\alpha,3p,1n$	8.9		
22–46	$3\alpha,1p$	36.6	2.52	3.09
21–45	$1\alpha,6p,4n$	−66.8		
21–45	$2\alpha,4p,2n$	−23.9		
21–45	$3\alpha,2p$	20.2	1.90	2.32
21–43	4α	30.9	2.40	2.94
20–43	$1\alpha,7p,5n$	−99.6		
20–43	$2\alpha,5p,3n$	−56.1		
20–43	$3\alpha,3p,1n$	−12.6		
20–42	$4\alpha,1p$	14.5		

IV. STATISTICAL-MODEL CALCULATIONS

A. The Monte Carlo computer code CACARIZO

Statistical-model calculations [1,4,58] have been found to be useful to simulate the competition between FF and FE (LP emission from a fully equilibrated CN). The following discussion addresses only the LP statistical decay from the

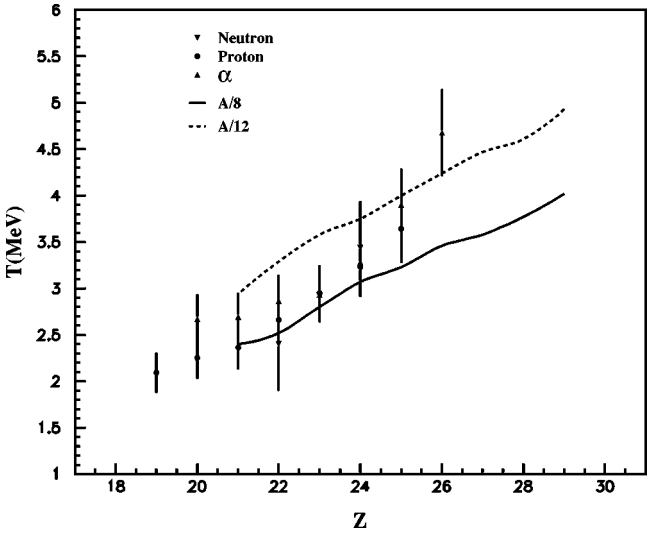

FIG. 10. Temperature of the emitter deduced from the LP energy spectra, as a function of its charge. The curves correspond to an estimated temperature for each emitter knowing the mean excitation energy carried away by each of the LPs (see text).

CN by comparison with the code CACARIZO [12,13,44]. CACARIZO is the Monte Carlo version [12] of the computer code CASCADE [58] and performs complete multistep calculations including an exact treatment of the spin coupling between the CN and the emitted LP. The CACARIZO code uses the Hauser-Feshbach formalism. It incorporates a semiclassical angular distribution, given by Ericson-Strutinski [59], to follow the whole evaporation chain of neutrons, proton, α particles, and finally the γ-ray emission until the cooling down is completed by the nucleus reaching the ground state. The use of a Monte Carlo code such as CACARIZO offers the opportunity to compare energy spectra in the laboratory frame, including a detailed account of experimental geometry and detector thresholds. Therefore the comparisons between experimental data and CACARIZO simulations are free from possible bias originating from the laboratory to c.m. frame transformation using average source velocity and emission angles. In the CACARIZO program [44] the CN is created with a given angular momentum and the deexcitation path is followed step by step and recorded in an event file. The different types of event (singles and/or coincidences) are then analyzed by taking into account the location and solid angles of the detectors.

B. Calculations procedures

The probability for a nucleus, with excitation energy E_1, angular momentum J_1, and parity π_1, to decay by evaporating a LP x with an orbital momentum l and kinetic energy ε_x in an energy bin $d\varepsilon_x$ and spin s is given by

$$P_x d\varepsilon_x = \frac{1}{\hbar}\Gamma(\varepsilon_x) = \frac{\rho_2(E_2,J_2,\pi_2)}{2\pi\hbar\rho_1(E_1,J_1,\pi_1)} \sum_{S=|J_2-s|}^{J_2+s} \sum_{\substack{l=|J_1-S| \\ [\pi]}}^{J_1+S} T_l(\varepsilon_x)d\varepsilon_x, \tag{5}$$

where E_2, J_2, and π_2 are the excitation energy, angular momentum, and parity of the daughter nucleus. ρ_1 and ρ_2 are, respectively, the level-density of the first excited fragment and the daughter nucleus. $\mathbf{S}=\mathbf{J}_2+\mathbf{s}$ is the channel spin. Finally $T_l(\varepsilon_x)$ are the transmission coefficients extracted from the inverse process by means of the standard OM potentials for elastic scattering. In the calculations of the OM transmission coefficients we used the parameters of Wilmore and Hodgson [61] for neutrons, Perey and Perey [62] for protons, and Huizenga and Igo [63] for α particles (see Table III).

C. Input parameters in CACARIZO

The two most basic quantities in statistical-model calculations are the nuclear level densities defining the available phase space and the transmission coefficients which control access to this phase space. Therefore the choice of their parametrizations plays a key role in the determination of the extent of the nuclear deformation and on possible dynamical effects for barrier reductions. For fast rotating nuclei, deformation effects may affect the emission barrier (and therefore T_l) of the LP and the level-density connected to the yrast line of the emitter. A complete self-consistent treatment of these effects through a particle cascade is a formidable and hard task, especially consuming CPU time. Some artificial means have been used in the code to attack this problem, as described below. The radius of the OM potential can be scaled by a factor to describe the effective potential barrier for the particle emission. The effective moment of inertia $\Im(J)$ of the emitter, which determines (at high excitation energy and high angular momentum) the spin dependence of the effective energy, is described in terms of the rigid-body moment of inertia. The rigid-body moment of inertia $\Im_{sphere}$ of a spherical nucleus with a radius parameter r_0 is taken to be that of a deformable liquid drop by assuming the deformability δ under rotation to be defined by the simple relation $\Im(J)=\Im_{sphere}(1+\delta J^2)$ [58], consistent with the RLDM of Cohen, Plasil, and Swiatecki [64]. In the present work the angular momentum dependence of the effective moment of inertia is taken into account in the CACARIZO calculations by the following modified formula [16,17,44]:

$$\Im(J) = \Im_{sphere}(1 + \delta_1 J^2 + \delta_2 J^4), \tag{6}$$

where δ_1 and δ_2 are the deformability parameters. This allows a large range of choices for the angular momentum dependence of the nuclear level densities. This moment of inertia is included in the following yrast line formula:

$$E_{rot}(J) = \frac{\hbar^2 J(J+1)}{2\Im(J)} + \Delta, \tag{7}$$

where Δ is the pairing energy of the emitter. By lowering the yrast line at high angular momentum we can increase the number of states in the phase space at higher angular momentum and hence decrease the emission of high-energy particles. This will be of great importance in trying to reproduce the energy spectra, especially for the α particles. For the level-density calculations, three regions have been taken into account:

TABLE III. Parameter sets for the evaporation calculations using CACARIZO for the $^{35}Cl+^{24}Mg$ reaction at $E_{lab}=260$ MeV.

Angular momentum distribution in CN
Critical angular momentum $L_{crit}=37\hbar$
Diffuseness parameter $\Delta l=1.0\hbar$
OM potentials of the emitted LCP and neutrons
(1) Neutrons: Wilmore and Hodgson (Ref. [61])
(2) Protons: Perey and Perey (Ref. [62])
(3) α particles: Huizenga and Igo (Ref. [63])
(4) Multiply factor of the OM radius: RFACT=1
Level-density parameters at low excitation: $E^*\leqslant 10$ MeV
(1) Fermi-gas level-density formula with empirical parameters from Dilg *et al.* (Ref. [67])
(2) Effective moment of inertia $\Im=(\mathrm{IFACT})\Im_{rigid}$ with IFACT=1
Level-density parameters at high excitation: $E^*\geqslant 15$ MeV
(1) Fermi-gas level-density formula with parameters from RLDM (Myers and Swiatecki [68])
(2) Level-density parameter $a=A/8$ MeV^{-1}
Yrast line
Parameter set *A*: RLDM (Cohen, Plasil, and Swiatecki [64])
Parameter set *B*: $\Im=\Im_{sphere}(1+\delta_1 J^2+\delta_2 J^4)$ with $\delta_1=1.1\times10^{-4}$ and $\delta_2=1.3\times10^{-7}$.
γ-ray width (Weisskopf units)
(1) $E1:B(E1)=0.001$
(2) $M1:B(M1)=0.01$
(3) $E2:B(E2)=5.0$

(1) Region I (low excitation energy, $E^*<4$ MeV): experimentally known discrete levels are introduced for each nucleus in the cascade. Furthermore high-spin states are also included in region II as yrast levels.

(2) Region II (medium excitation energy, 4 MeV$<E^*<10$ MeV): the level-density is determined from the angular momentum dependent level-density formula for a spherical nucleus given by Lang [65]. The excitation energy is corrected for the parity effects. The level-density parameter a and Δ are deduced empirically for each nucleus from the compilations proposed by Vonach and Hille [66] and Dilg *et al.* [67].

(3) Region III (high excitation energy, $E^*>E_{RLDM}\simeq 15$ MeV): shell effects and parity corrections are neglected in this region. The same formula is then used but with RLDM parameters [68].

Between regions II and III the level-density parameters are interpolated linearly. The two parameter sets used for the calculation are summarized in Table III.

D. Discussion of the influence of the parameters in CACARIZO

A systematic study of the sensitivity to the choice of parameters in CACARIZO is presented in this section. The most sensitive parameters influencing the calculated LP energy spectra in coincidence with the ERs are the critical angular momentum L_{crit}, the diffusivity parameter Δl, the level-density parameter a, the nuclear radius parameter r_0, the transmission coefficients T_l, and the deformability parameters δ_1 and δ_2. Figure 11 shows the energy spectra of α particles detected at $\theta_{LCP}=+30°$ in coincidence with the ERs ($18\leqslant Z\leqslant 24$) at $\theta_{ER}=-10°$ which are compared with the CACARIZO predictions using several choices of parameter.

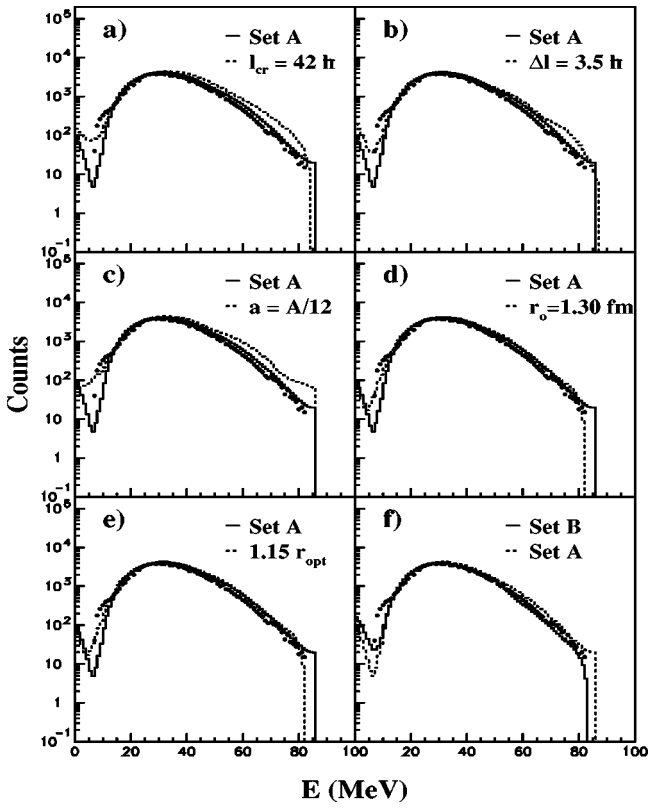

FIG. 11. Kinetic energy spectra of α particles measured at $\theta_{LCP}=+30°$ in coincidence with ERs detected in-plane at $\theta_{ER}=-10°$ for the $^{35}Cl+^{24}Mg$ reaction. The full histograms and dashed histograms are the results of statistical-model calculations using CACARIZO with different parameter sets as discussed in the text.

1. Critical angular momentum

Usually the L_{crit} values are derived from the CF cross section data, when available, using the sharp cutoff approximation. For the ^{35}Cl (260 MeV)$+^{24}Mg$ reaction under study, the choice of the L_{crit} value has been determined from the extrapolation of earlier inclusive measurements performed for the same reaction at two neighboring bombarding energies $E_{lab}=278$ MeV [7,11] and $E_{lab}=282$ MeV [5,6] with $L_{crit}=37\hbar$ and $39\hbar$, respectively. The value of $L_{crit}=37\hbar$ has been selected finally to be more consistent for the present bombarding energy. However to check the sensitivity of the CACARIZO calculations to the critical angular momentum, two different L_{crit} values ($L_{crit}=37\hbar$ and $42\hbar$) have been used [see Fig. 11(a)]. The $L_{crit}=37\hbar$ calculation is shown by the solid line whereas the $L_{crit}=42\hbar$ calculation is shown by the dashed line. The other parameter values are those from the set *A* given in Table III. The shapes of the experimental energy spectra [see Fig. 11(a)] are relatively well described by both calculations although their high-energy tails become

harder than observed experimentally. The discrepancy is found to be larger for the higher L_{crit} value with the maximum shifted to slightly higher energy, whereas the spectrum broadened at high energy as found previously for the $^{30}Si+^{30}Si$ reaction [19]. At higher angular momentum the yrast line is too steep, making the level-density too low, and therefore the emission of high-energy particles is overly favored.

2. Diffuseness parameter

Increasing the value of the diffuseness parameter of the angular momentum distribution has the same consequences as increasing the L_{crit} value. From the results shown in Fig. 11(b) for $\Delta l=1\hbar$ (full line) and $\Delta l=3.5\hbar$ (dashed line), it can be concluded that the larger value induces too much yield for the high-energy tail of the spectrum. It is known from the systematics [58] that this parameter value is usually kept between $\Delta l=0.71\hbar$ and $\Delta l=1.3\hbar$ for the light systems of interest, and about $\Delta l=3.5\hbar$ for the heaviest one. In a recent treatment made by the Legnaro group [13,14] the value of $3.5\hbar$ has been used for the same CN using the $^{32}S+^{27}Al$ entrance channel; however the reason for this particular choice was not discussed [13,14]. From our previous investigations of the $^{35}Cl+^{12}C$ [3] and the $^{35}Cl+^{24}Mg$ [5–11] reactions, and following systematic studies in the $20\leqslant A\leqslant 60$ mass region [1,4] the value of $1\hbar$ has been finally adopted. This low value appears to be consistent with the choice of $\Delta l=2\hbar$ for this parameter for heavier systems [16,17,23,69,70].

3. Level-density parameter

The influence of the level-density parameter a on the predicted spectra is displayed in Fig. 11(c), where the calculated spectra obtained with two values of a are shown: $a=A/8$ as the full line and $a=A/12$ as the dashed line. An increase in yield is found in the high-energy tail of the α-particle spectrum as soon as the value of the level-density parameter is decreased. This can be understood by the simple fact that the level-density is exponentially proportional to the square root of a. This will reduce the level-density when we reduce a and hence energetic particle emission will be favored. A reasonable choice of the parameter a has to be made with great care. There is an experimental indication in this work leaning towards $a=A/8$. A higher value of a is needed to reproduce the experimental spectrum, in contrast with several works and predictions for this region of mass and excitation energy, as detailed below. The value of this parameter is about $a=A/15$ within a Fermi-gas approach for the heavy systems with $A>100$. Recently the temperature dependence of a has been investigated ($A/13<a<A/8$ when $T\approx 4-5$ MeV) [48–51]. Nicolis *et al.* [71] have introduced an analytical temperature-dependent parametrization of a, where thermal and quantal fluctuations are taken into account. This parametrization is in good agreement with the predictions of Ref. [55]. A modest energy dependence of the level-density parameter has been proved, both theoretically [55] and more recently experimentally [56]. The a parameter value is also affected by dynamical deformation, rotation induces rearrangement of the single-particle level scheme, and by the macroscopic effects of the altered nuclear surface [17]. The a parameter is found to increase when the deformation increases [57]. The situation is rather simpler for light heavy ions, and the investigation of the level-density for hot nuclei with mass $A<40$ has been performed systematically [20]. From this study a value of $a=A/8$ seems to be reasonable, as shown in Sec. III B. Finally a value of $a=A/8$ is selected in agreement with earlier studies [17,20], the theoretical studies of Shlomo and Natowitz [55] or Töke and Swiatecki [57] and experimental results obtained very recently in the mass 60 region [28].

4. Nuclear radius parameter

The variation of the nuclear radius parameter r_0, used in the moment-of-inertia calculation within the RLDM parametrization, has no significant effect on the calculations as shown in Fig. 11(d). The two calculations were performed with $L_{crit}=37\hbar$, $\Delta l=1\hbar$, and $a=A/8$. The first calculated spectrum (full line) assumes a radius given by the Myers and Swiatecki formula [72]; the second (dashed line) was obtained with the constant value $r_0=1.30$ fm. We note that a similar value ($r_0=1.28$ fm) was used by Huizenga *et al.* [17] for an exhaustive investigation of the $^{32}S+^{27}Al$ reaction. Myers and Swiatecki parametrizations were used for a realistic interpretation of the nuclear radius parameter, due to the similarity between the two calculations.

5. Transmission coefficients

The transmission coefficients T_l are calculated by considering the potentials (generally the OM potentials given in Table III) describing the inverse reaction on cold nuclei, with the assumption that the emission barriers for cold nuclei and hot nuclei are identical. Earlier studies concerning the same mass region [12–15,44] have indicated that it is helpful to reduce the emission barrier of the LP to get good agreement between the experimental and the calculated spectra. The CACARIZO code used here, in common with many others, does not allow us a full description of either the shape of the emitter at given excitation energy and angular momentum or the position from where the LP is emitted. A complete self-consistent treatment of these effects through a particle cascade is a formidable and hard task. An artificial means has been used in the present code to disentangle this problem. The radius of the OM potential has been scaled by a factor (greater than unity to decrease the LP emission barrier) in order to describe the effective potential barrier for the particle emission. A detailed study of the T_l parameters has been undertaken by the group of Huizenga [17], by using three different shapes: spherical, oblate, and prolate. The study has taken into account a mean value of a weighted $T_l(R)$ over all the surface. The weighting allows the emission direction to be introduced classically relative to the emitter spin of the LP. The results and the conclusions given in this work support that the emission barrier is insensitive to the shape of the emitter whether it is spherical or deformed. It should be noted that this weight is non-spin-dependent and does have some consequences. The results from these two kinds of approach are shown in Fig. 11(e), where a calculation per-

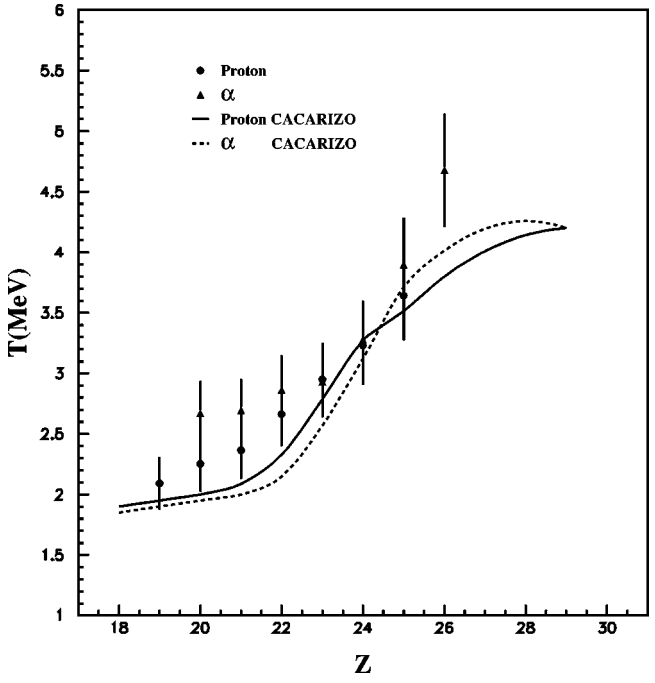

FIG. 12. Temperature of the emitter deduced from the energy spectra of protons and α particles, as a function of its charge (see Fig. 10). The curves correspond to the temperature extracted from the energy spectra calculated using CACARIZO.

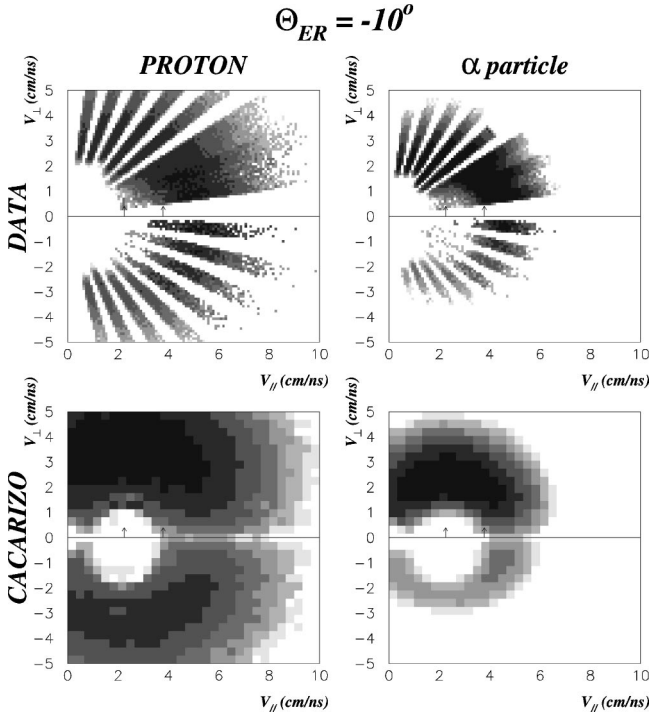

FIG. 13. Exclusive proton and α-particle Galilean-invariant cross sections. Upper part measured in coincidence with the ERs ($18 \leqslant Z \leqslant 24$) for the ^{35}Cl+^{24}Mg reaction. Galilean-invariant cross sections are plotted as a function of the perpendicular and parallel velocities with respect to the beam axis. Lower part: the same plots as obtained from CACARIZO.

formed with spherical parameters for the T_l parameters (solid line) and with the radius increased by 15% (dashed line) is shown. The larger radius increases the low-energy LP. This artifice to lower the emission barrier of the LP has been extensively criticized. Using this method in our analysis is not justified (at this moment) when T_l parameters derived from a spherical nucleus are sufficient to reproduce the energy spectra of α particles. It is worth noting, however, that for hot heavy nuclei at high excitation energy a lowering of the α-particle emission barrier has to be taken into account [73].

6. Deformability parameters

The last input parameters capable of lowering the contribution from high-energy α particles and hence getting improved agreement with the experimental data are those of the deformability. In fact until now the spin-dependent moment of inertia has been taken into account in the calculation so as to be consistent with the deformation of a liquid drop (RLDM [64]), i.e., with very small values given to deformability parameters ($\delta_1 = 7.6 \times 10^{-6}$ and $\delta_2 = 6.7 \times 10^{-8}$). It is noted that a lowering of the entrance channel critical angular momentum could remove the disagreement, but the value of $L_{crit} = 37\hbar$ is imposed experimentally. We have already mentioned that increasing the moment of inertia (according to the spin) decreases the slope of the yrast line at higher spin and hence increases the phase space available when emitting α particles with lower energies. To obtain good agreement with the α-particle energy spectra, increased values of $\delta_1 = 1.1 \times 10^{-4}$ and $\delta_2 = 1.3 \times 10^{-7}$ have been selected. As shown in Fig. 11(f) the calculation with this last parametrization (solid line) reproduces the experimental data very well.

E. Nuclear temperature estimations with CACARIZO

The extraction of NTPs, from the calculated LCP energy spectra in the ^{59}Cu frame (using the parameter set *B*) of the LCP, has been attempted. The comparison is shown in Fig. 12 where the data are plotted as solid points for the protons and solid triangles for α particles. The results extracted from the calculations are presented by a solid line for the protons and a dashed line for α particles. Satisfactory agreement within the errors bars (including systematic uncertainties of $\approx$10%) is obtained. It should be noted that the small disagreement at $Z \leqslant 22$ can be explained by the fact that the NTPs were extracted experimentally [10] from the energy spectra of the LCP in the frame of the parent emitter (where the LCP in coincidence with the ER was assumed to be the last one emitted in the cascade).

F. Analysis of the experimental results with CACARIZO

The experimental Galilean-invariant cross section maps ($V_{\parallel}$-$V_{\perp}$) are presented in Fig. 13 for both the protons and the α particles (top). Results obtained using CACARIZO are also shown (bottom). A qualitative agreement is found. The discontinuity at 0° is due to the fact that the test of coplanarity is more difficult in the analysis program when the sine of the

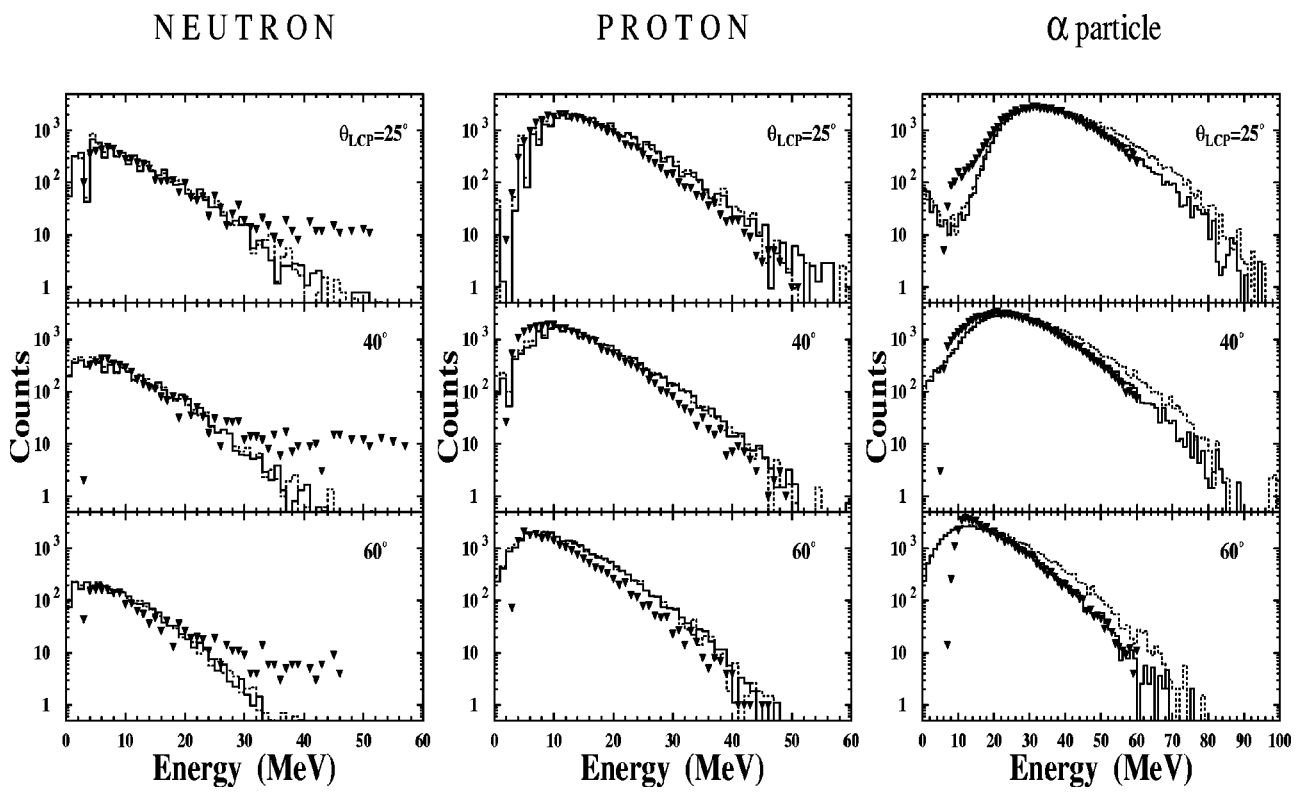

FIG. 14. Energy spectra of the neutrons, protons, and α particles detected in-plane at the indicated angles, in coincidence with the ERs ($18 \leqslant Z \leqslant 24$) emitted at $\theta_{ER}=-10°$. The full and dashed line histograms correspond to the results obtained with CACARIZO using parameter sets *B* and *A*, respectively.

angle is close to zero. Due to the reverse kinematics used in this experiment the ERs are essentially forward peaked and the CACARIZO calculations are only meaningful for the particles emitted in coincidence with the ERs detected at $\theta_{lab}=-10°$.

In Fig. 14 the results of the code with both parameter sets are compared to the experimental energy spectra of neutrons, protons, and α particles at the indicated angles. The first result from the comparison is that the neutron spectra are well reproduced by both parameter sets. This is due to the fact that neutrons do not remove large amounts of angular momentum and are not subject to the emission barrier. Note that the tail (for experimental data) at high energy is due to the difficult discrimination (TOF—total representation) between the energetic neutrons (low TOF) and the γ-ray component. The second observation is for the protons where both parameter sets fail to give a satisfactory reproduction of the data. The emission barrier and the high-energy yields are overestimated. This result concerning the emission barrier is consistent with the usual observations in the literature concerning the evaporation of LP (see Refs. [13,70]). The problem is related to the computation of the T_l coefficients in the OM. This is a very delicate task for the protons [23,70], essentially due to the problems of transparency and absorption of the protons in the OM in contrast with the α-particle situation (as to be seen later). A recent alternative treatment called IWBCM [74], which takes into account only the real part of the potential (transparency is neglected), can give a good reproduction [23,70] of the production cross section of the protons. This kind of treatment should be tried in the future with the CACARIZO code. The third observation is that the neutron and proton spectra are insensitive to the lowering of the yrast line at high angular momentum whereas this is not the case for α particles. The calculation using parameter set *A*, in which the moment of inertia is calculated using RLDM parameters, overestimates the higher-energy part of the α-particle spectra. This disagreement is removed when a deformation is introduced by increasing the deformability parameters (δ_1 and δ_2, see Sec. IV D 6). This implies a deformation ratio of $b/a=1.65$ or $b/a=1.74$ (where *b* and *a* are the major and minor axes and *c* is the rotational axis of the ellipsoidal CN) assuming, respectively, an oblate or a prolate shape for the CN. The emission barrier and the slope at high energy of the α-particle spectra are well reproduced with the parameter set *B*. A small disagreement remains at low energy, probably due to the overestimation of the emission barrier.

It is interesting to notice that the coincident energy spectra of neutrons, protons, and α particles detected out of plane (see Fig. 15) are well reproduced with both *parameter sets* in contrast with the in-plane correlation. This confirms that the calculations are properly reproducing the experimental data. The comparison of the experimental angular correlation with the calculations is shown in Fig. 16. The in-plane and out-of-plane correlations are given for neutrons, protons, and α particles. The two sets of results have been normalized by the same normalization factor. The normalizations for each particle type have been done independently. The two calculations each reproduce the shape of the correlations in a satisfactory manner. This is especially true for the neutrons,

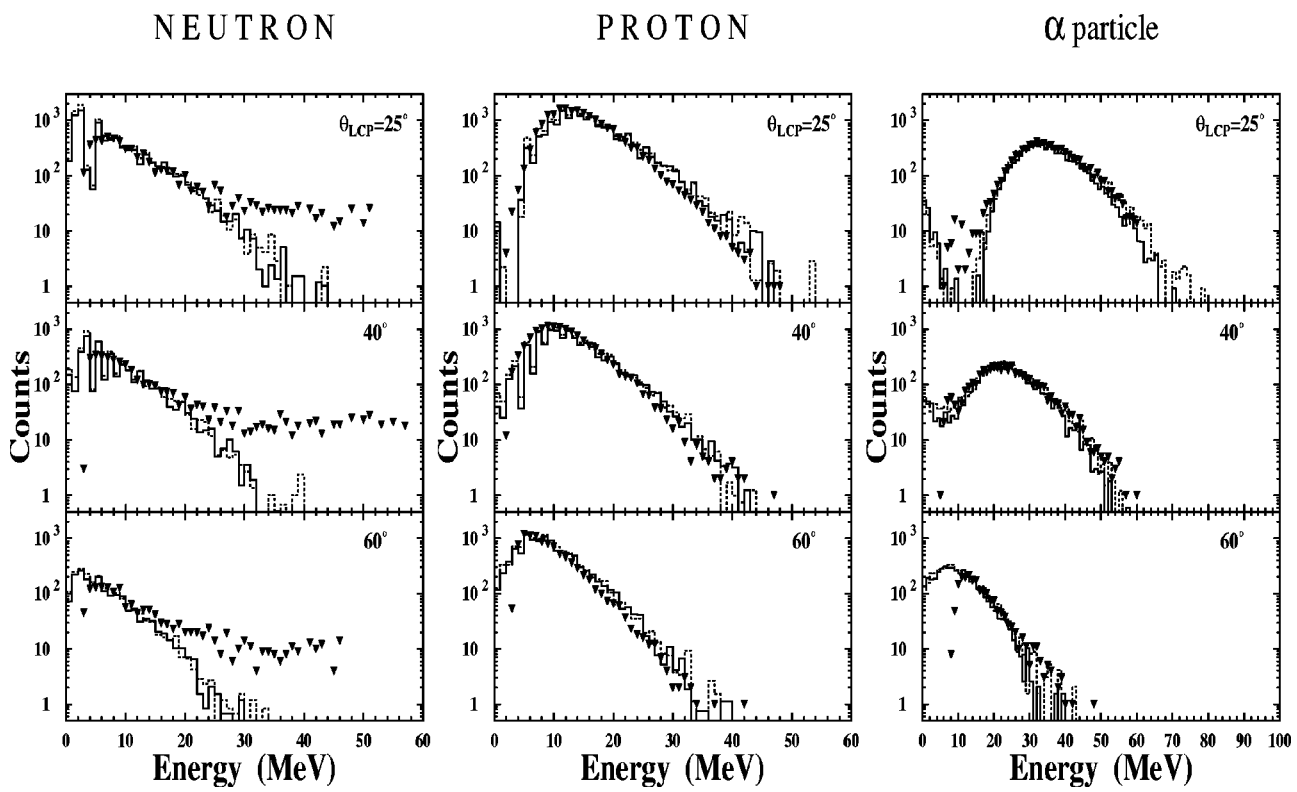

FIG. 15. Energy spectra of the neutrons, protons, and α particles detected at the indicated angles, in coincidence with the ERs ($18 \leqslant Z \leqslant 24$) emitted out of plane at $\theta_{ER}=10°$. The full and dashed line histograms correspond to the results obtained with CACARIZO using parameter sets *B* and *A*, respectively.

which are not perturbed by the Coulomb repulsion. Note that the emission barrier of the α particles is more or less reproduced in the energy spectra. The same conclusion can be advanced for the maximum in the in-plane angular correlation. A significant discrepancy for the maximum is found in the in-plane proton angular correlations. This disagreement is possibly related to an overestimation of the emission barrier for the protons (see the energy spectra). This hypothesis can be supported by the neutron and α-particle correlations where the Coulomb repulsion is zero for neutrons and is well reproduced for the α particles. This is probably not the only reason for the shift between the data and the calculations. We have tried several parameters to tackle the problem, nevertheless this problem remains an open question.

The experimental anisotropy factor is not well reproduced by the calculations for either the proton or the α-particle out-of-plane correlations. On the other hand, the statistical-model code is able to reproduce the neutron out-of-plane angular correlations within the error bars. The angular momentum dependence has been tested by performing calculations with three different angular momentum windows: $(10-20)\hbar$, $(20-30)\hbar$, and $(30-37)\hbar$. Whereas for neutrons and protons the anisotropy is almost constant with the *L* window [75], for the α particles the anisotropy is strongly dependent on the chosen *L* window. Nevertheless the flat behavior shown around 0° is present for the three particle species. In an attempt to understand this problem, more accuracy has been demanded by using more exclusive data. In Fig. 17 the in-plane and out-of-plane angular correlations are reported for both protons and α particles in coincidence with ERs with charge $Z=21$, 22, and 23. The data are compared to the calculations using parameter set *B*. The same conclusions can be drawn as for the early less constrained comparison. This is true also for the in-plane angular correlations. The origin of this discrepancy in the angular correlations might be understood by further investigations into the emission barrier of the LCP for the in-plane correlation. Concerning the out-of-plane angular correlations we possibly need to use a more complete formulation for the angular distribution of the LP which is treated in a semiclassical way.

V. SUMMARY AND CONCLUSIONS

In-plane and out-of-plane light charged particle and neutron correlations in coincidence with evaporation residues produced in the ^{35}Cl (260 MeV) + ^{24}Mg fusion reaction have been measured to investigate deformation and angular momentum effects of the decaying ^{59}Cu compound nucleus. An array of 21 BaF_2 crystals has been used to identify both the light charged particles ($Z \leqslant 4$) and the neutrons emitted in coincidence with heavy fragments ($Z \geqslant 5$) detected in six ionization chamber telescopes. Coincident energy spectra and Galilean-invariant cross section plots have shown the statistical character of the deexcitation of the CN and its ERs, as well as the absence of any observable preequilibrium emission of the LPs (i.e., ICF has small cross sections [6,8]), which is negligible compared to CF. These statements justi-

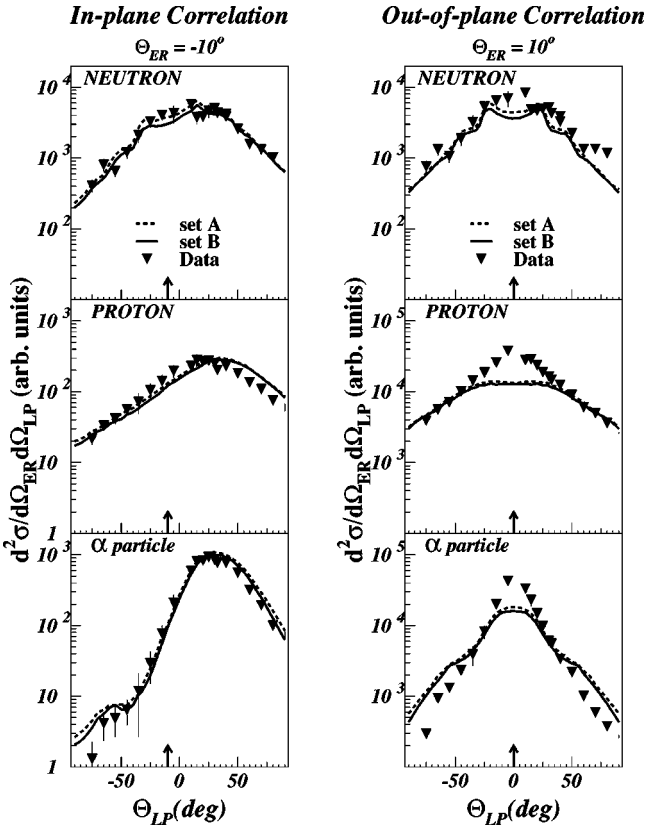

FIG. 16. In-plane and out-of plane angular correlations for neutrons, protons, and α particles detected in coincidence with the ERs ($18 \leqslant Z \leqslant 24$) emitted at $\theta_{lab} = 10°$. The arrows indicate the emission angle of the ERs. The full and dashed lines correspond to the results obtained with CACARIZO using parameter sets *B* and *A*, respectively.

fied the use of a statistical-model code to compare with the experimental results.

Coincident energy spectra and angular distributions of neutrons, protons, and α particles have been compared to a statistical-model description. The statistical-model calculations have been performed using the Monte Carlo code CACARIZO with adjusted nuclear level densities. The NTP extracted from the energy spectra of the LPs was crucial in fixing the nuclear level-density parameter at a value of $A/8$. The comparisons between the experimental results and the code are satisfactory and lead to the conclusion that a large deformation is required to reproduce the energy spectra of the α particles, which were the most sensitive. Nevertheless there is still work to be done within CACARIZO to resolve some remaining problems, especially the problem of the emission barrier of the protons and general problems with the angular distribution of the LP with respect to the spin of the emitter. The method has shown its validity and/or usefulness as a tool to investigate the deformation of nuclei. It can be used in a complementary fashion to the spectroscopy. This tool has recently been used to investigate the deformation of the ^{40}Ca [33,37], ^{44}Ti [34–37], and ^{56}Ni [32,37] nuclei.

The large deformation needed to reproduce the energy spectra of the α particles supports the fact that the CN is extremely deformed and can undergo the FF process even in this light heavy-ion mass region ($A \leqslant 60$). This means that this process should be included in the various statistical-model codes treating the reaction mechanisms, already included in the transition state model [1] as well as in the extended Hauser-Feshbach method [4]. Work is in progress to describe in a similar manner the light charged particle and neutron data as measured in coincidence with the binary fragments.

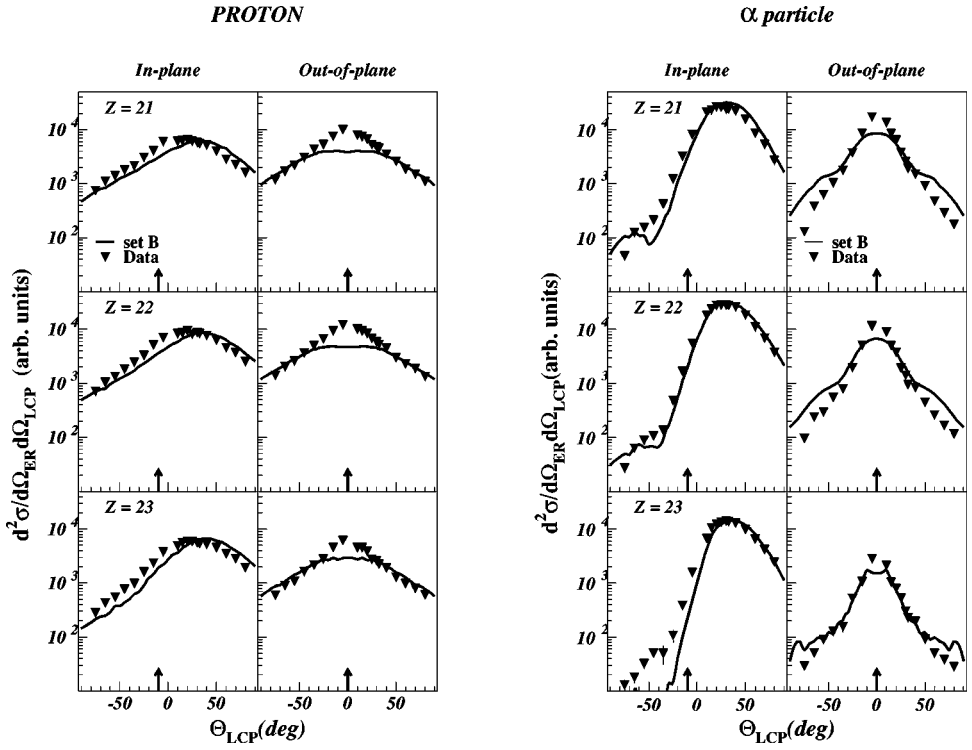

FIG. 17. In-plane and out-of plane angular correlations for protons and α particles detected with ERs having $Z = 21$, 22, and 23. The arrows indicate the emission angle of the ERs. The full lines correspond to the results obtained with CACARIZO using the parameter set *B*.

ACKNOWLEDGMENTS

This paper is based upon the Ph.D. thesis of D. Mahboub, Université Louis Pasteur, Strasbourg, 1996. The authors wish to thank the Post-accelerator Tandem Service at Saclay for their warm hospitality and technical support. Three of us (D.M., C.B., and Sl.C.) wish also to acknowledge Dr. G. Viesti for helping us to perform the first attempts of statistical-model calculations using CACARIZO. D.M. wishes to thank the INFN and the University of Surrey (EPSRC) for their financial support which allowed him to finish the paper. He also wishes to thank Dr. W. Catford and Professor W. Gelletly for their useful discussions and for a careful reading of the manuscript.

[1] S. J. Sanders, A. Szanto de Toledo, and C. Beck, Phys. Rep. **311**, 487 (1999); and references therein.
[2] C. Beck and A. Szanto de Toledo, Phys. Rev. C **53**, 1989 (1996).
[3] C. Beck, D. Mahboub, R. Nouicer, T. Matsuse, B. Djerroud, R. M. Freeman, F. Haas, A. Hachem, A. Morsad, M. Youlal, S. J. Sanders, R. Dayras, J. P. Wieleczko, E. Berthoumieux, R. Legrain, E. Pollacco, Sl. Cavallaro, E. De Filippo, G. Lanzanò, A. Pagano, and M. L. Sperduto, Phys. Rev. C **54**, 227 (1996).
[4] T. Matsuse, C. Beck, R. Nouicer, and D. Mahboub, Phys. Rev. C **55**, 1380 (1997).
[5] Sl. Cavallaro, C. Beck, E. Berthoumieux, R. Dayras, E. De Filippo, E. Di Natale, B. Djerroud, R. M. Freeman, A. Hachem, F. Haas, B. Heusch, G. Lanzanò, R. Legrain, D. Mahboub, A. Morsad, A. Pagano, E. Pollacco, S. J. Sanders, and M. L. Sperduto, Nucl. Phys. **A583**, 161 (1995).
[6] Sl. Cavallaro, E. De Filippo, G. Lanzanò, A. Pagano, M. L. Sperduto, R. Dayras, R. Legrain, E. Pollacco, C. Beck, B. Djerroud, R. M. Freeman, F. Haas, A. Hachem, B. Heusch, D. Mahboub, A. Morsad, R. Nouicer, and S. J. Sanders, Phys. Rev. C **57**, 731 (1998).
[7] R. Nouicer, C. Beck, D. Mahboub, T. Matsuse, B. Djerroud, R. M. Freeman, A. Hachem, Sl. Cavallaro, E. De Filippo, G. Lanzanò, A. Pagano, M. L. Sperduto, R. Dayras, E. Berthoumieux, R. Legrain, and E. Pollacco, Z. Phys. A **356**, 5 (1996).
[8] C. Beck, R. Nouicer, D. Mahboub, T. Matsuse, B. Djerroud, R. M. Freeman, A. Hachem, Sl. Cavallaro, E. De Filippo, G. Lanzanò, A. Pagano, M. L. Sperduto, R. Dayras, E. Berthoumieux, R. Legrain, and E. Pollacco, Eur. Phys. J. A **2** 281 (1998).
[9] C. Beck, D. Mahboub, B. Djerroud, R. M. Freeman, F. Haas, A. Hachem, Sl. Cavallaro, E. De Filippo, E. Di Natale, G. Lanzanò, A. Pagano, M. L. Sperduto, R. Dayras, E. Berthoumieux, R. Legrain, and E. Pollacco, Ric. Sci. ed Educazione Permanente (Suppl.) 101, 127 (1995).
[10] D. Mahboub, Ph.D. thesis, Strasbourg University, 1996.
[11] R. Nouicer, Ph.D. thesis, Strasbourg University, 1997.
[12] R. K. Choudhury, P. L. Gonthier, K. Hagel, M. N. Namboodiri, J. B. Natowitz, L. Adler, S. Simon, S. Kniffen, and G. Berkowitz, Phys. Lett. **143B**, 74 (1984).
[13] G. Viesti, B. Fornal, D. Fabris, K. Hagel, J. B. Natowitz, G. Nebbia, G. Prete, and F. Trotti, Phys. Rev. C **38**, 2640 (1988).
[14] B. Fornal, G. Prete, G. Nebbia, F. Trotti, G. Viesti, D. Fabris, K. Hagel, and J. B. Natowitz, Phys. Rev. C **37**, 2624 (1988); **40**, 664 (1989).
[15] B. Fornal, F. Gramegna, G. Prete, R. Burch, G. D'Erasmo, E. M. Fiore, L. Fiore, A. Pantaleo, V. Paticchio, G. Viesti, P. Blasi, N. Gelli, F. Lucarelli, M. Anghinolfi, P. Corvisiero, M. Taiuti, A. Zucchiatti, P. F. Bortignon, J. Ruiz, G. Nebbia, M. Gonin, and J. B. Natowitz, Phys. Lett. B **255**, 325 (1991).
[16] I. M. Govil, J. R. Huizenga, W. U. Schroder, and J. Töke, Phys. Lett. B **197**, 515 (1987).
[17] J. R. Huizenga, A. N. Behkami, I. M. Govil, W. U. Schröder, and J. Töke, Phys. Rev. C **40**, 668 (1989).
[18] G. La Rana, R. Moro, A. Brondi, P. Cuzzocrea, A. D'Onofrio, E. Perillo, M. Romano, F. Terrasi, E. Vardaci, and H. Dumont, Phys. Rev. C **37**, 1920 (1988); **40**, 2425 (1989).
[19] N. G. Nicolis and D. G. Sarantites, Phys. Rev. C **40**, 2422 (1989).
[20] B. Fornal, F. Gramegna, G. Prete, R. Burch, G. D'Erasmo, E. M. Fiore, L. Fiore, A. Pantaleo, V. Paticchio, G. Viesti, P. Blasi, M. Cinausero, F. Lucarelli, M. Anghinolfi, P. Corvisiero, M. Taiuti, A. Zucchiatti, P. F. Bortignon, D. Fabris, G. Nebbia, and J. A. Ruiz, Phys. Rev. C **44**, 2588 (1991).
[21] D. K. Agnihotri, A. Kumar, K. C. Jain, K. P. Singh, G. Singh, D. Kabiraj, D. K. Avasthi, and I. M. Govil, Phys. Lett. B **307**, 283 (1993).
[22] M. F. Vineyard, S. E. Atencio, J. F. Crum, G. P. Gilfoyle, B. G. Glagola, D. J. Henderson, D. G. Kovar, C. F. Maguire, J. F. Mateja, R. G. Ohl, F. W. Prosser, J. H. Rollinson, and R. S. Trotter, Phys. Rev. C **49**, 948 (1994).
[23] M. Kildir, G. La Rana, R. Moro, A. Brondi, E. Vardaci, A. D'Onofrio, D. Fessas, E. Perillo, V. Roca, M. Romano, F. Terrasi, G. Nebbia, G. Viesti, and G. Prete, Phys. Rev. C **51**, 1873 (1995).
[24] F. Bourgine, D. Cabaussel, D. Boivin, M. Aiche, M.-M. Aleonard, G. Barreau, J.-F. Chemin, T. P. Doan, J. P. Goudour, M. Harston, J.-N. Scheurer, A. Brondi, G. La Rana, R. Moro, A. Principe, E. Vardaci, and D. Curien, Phys. Rev. C **56**, 3180 (1997).
[25] I. M. Govil, R. Singh, A. Kumar, J. Kaur, A. K. Sinha, N. Madhavan, D. O. Kataria, P. Sugathan, S. K. Kataria, K. Kumar, B. John, and G. V. Ravi Prasad, Phys. Rev. C **57**, 1269 (1998).
[26] D. Bandyopadhyay, S. K. Basu, C. Bhattacharya, S. Bhattacharya, K. Krishan, A. Chatterjee, S. Kailas, A. Navin, and A. Srivastava, Phys. Rev. C **59**, 1179 (1999).
[27] C. Bhattacharya, M. Rousseau, C. Beck, V. Rauch, R. Nouicer, R. M. Freeman, O. Stezowski, D. Mahboub, S. Belhabib, A. Hachem, A. Dummer, S. J. Sanders, and A. Szanto de Toledo, Nucl. Phys. **A654**, 841c (1999).
[28] P. Jänker, H. Leitz, K. E.G. Löbner, M. Morales, and H. G. Thies, Eur. Phys. J. A **4**, 147 (1999).
[29] I. M. Govil, R. Singh, Ajay Kumar, A. Kumar, G. Singh, S. K. Kataria, and S. K. Datta, Phys. Rev. C **62**, 064606 (2000).
[30] I. M. Govil, R. Singh, A. Kumar, S. K. Datta, and S. K. Kataria, Nucl. Phys. **A674**, 377 (2000).

[31] D. Bandyopadhyay, C. Bhattacharya, K. Krishan, S. Bhattacharya, S. K. Basu, A. Chatterjee, S Kailas, A. Srivastava, and K. Mahata, Phys. Rev. C **64**, 064613 (2001); Eur. Phys. J. A **14**, 53 (2002).

[32] C. Bhattacharya, M. Rousseau, C. Beck, V. Rauch, R. M. Freeman, D. Mahboub, R. Nouicer, P. Papka, O. Stezowski, A. Hachem, E. Martin, A. K. Dummer, S. J. Sanders, and A. Szanto De Toledo, Phys. Rev. C **65**, 014611 (2002).

[33] M. Rousseau, C. Beck, C. Bhattacharya, V. Rauch, O. Dorvaux, K. Eddahbi, C. Enaux, R. M. Freeman, F. Haas, D. Mahboub, R. Nouicer, P. Papka, O. Stezowski, S. Szilner, A. Hachem, E. Martin, S. J. Sanders, A. K. Dummer, and A. Szanto de Toledo, Phys. Rev. C **66**, 034612 (2002).

[34] C. Beck, M. Rousseau, P. Papka, A. Sánchez i Zafra, C. Bhattacharya, V. Rauch, P. Bednarczyk, S. Courtin, O. Dorvaux, F. Haas, R. Nouicer, A. Nourreddine, I. Piqueras, J. Robin, S. Szilner, O. Stezowski, A. Prévost, S. Thummerer, W. von Oertzen, A. Hachem, E. Martin, A. Fahli, A. Morsad, A. Szanto de Toledo, and S. J. Sanders, in *Proceedings of the Symposium on Nuclear Clusters*, edited by R. Jolos and W. Scheid (EP Systema, Debrecen, Hungary, 2003), p. 171.

[35] P. Papka, C. Beck, M. Rousseau, A. Sánchez i Zafra, C. Bhattacharya, V. Rauch, P. Bednarczyk, O. Dorvaux, F. Haas, A. Nourreddine, I. Piqueras, J. Robin, S. Szilner, O. Stezowski, A. Prévost, S. Thummerer, W. von Oertzen , A. Fahli, and A. Morsad, Acta Phys. Pol. B **34**, 2343 (2003).

[36] P. Papka, C. Beck, F. Haas, V. Rauch, M. Rousseau, P. Bednarczyk, S. Courtin, O. Dorvaux, K. Eddahbi, I. Piqueras, K. Kezzar, J. Robin, A. Sànchez i Zafra, S. Thummerer, A. Hachem, E. Martin, N. Redon, B. Rossé, O. Stézowski, A. Prévost, and A. Wuosmaa, in *Proceedings of the Tenth Varenna Conference on Nuclear Reaction Mechanisms, Varenna, 2003*, edited by E. Gadioli [Ricerca Scientifica ed Educazione Permanente (Suppl.) 122, 373 (2003)].

[37] C. Beck, Int. J. Mod. Phys. E (to be published); nucl-th/0401005.

[38] C. Andreoiu, D. Rudolph, C. E. Svensson, A. V. Afanasjev, J. Dobaczewski, I. Ragnarsson, C. Baktash, J. Eberth, C. Fahlander, D. S. Haslip, D. R. LaFosse, S. D. Paul, D. G. Sarantites, H. G. Thomas, J. C. Waddington, W. Weintraub, J. N. Wilson, and C.-H. Yu, Phys. Rev. C **62**, 051301 (2000).

[39] C. Andreoiu, D. Rudolph, I. Ragnarsson, C. Fahlander, R. A. E. Austin, M. P. Carpenter, R. M. Clark, J. Ekman, R. V. F. Janssens, T. L. Khoo, F. G. Kondev, T. Lauritsen, T. Rodinger, D. G. Sarantites, D. Seweryniak, T. Steinhardt, C. E. Svensson, O. Thelen, and J. C. Waddington, Eur. Phys. J. A **14**, 317 (2002).

[40] D. Rudolph, C. Andreoiu, C. Fahlander, R. J. Charity, M. Devlin, D. G. Sarantites, L. G. Sobotka, D .P. Balamuth, J. Eberth, A. Galindo-Uribarri, P. A. Hausladen, D. Seweryniak, and Th. Steinhardt, Phys. Rev. Lett. **89**, 022501 (2002).

[41] C. Andreoiu, T. Dossing, C. Fahlander, I. Ragnarsson, D. Rudolph, S. Aberg, R. A. E. Austin, M. P. Carpenter, R. M. Clark, R. V. F. Janssens, T. L. Khoo, F. G. Kondev, T. Lauritsen, T. Rodinger, D. G. Sarantites, and D. Seweryniak, Phys. Rev. Lett. **91rm**, 232502 (2003).

[42] J. Dobaczewski, J. Dudek, and R. Wyss, Phys. Rev. C **67**, 034308 (2003).

[43] W. Z. Jiang, T. T. Wang, and Z. Y. Zhu, Phys. Rev. C **68**, 047301 (2003).

[44] Z. Majka, M. E. Brandan, D. Fabris, K. Hagel, A. Menchaca-Rocha, J. B. Natowitz, G. Nebbia, G. Prete, B. Sterling, and G. Viesti, Phys. Rev. C **35**, 2125 (1987).

[45] G. Lanzanò, A. Pagano, E. de Filippo, B. Berthier, J. L. Charvet, R. Dayras, R. Legrain, R. Lucas, C. Mazur, E. Pollacco, J. E. Sauvestre, C. Volant, C. Beck, B. Djerroud, and B. Heusch, Nucl. Instrum. Methods Phys. Res. A **312**, 515 (1992); **332**, 161 (1993); **342**, 627 (1997).

[46] G. Lanzanò, E. de Filippo, M. Geraci, A. Pagano, S. Urso, N. Colonna, G. D'Erasmo, E. M. Fiore, and A. Pantaleo, Nuovo Cimento Soc. Ital. Fis., A **110A**, 505 (1997).

[47] J. Gomez del Campo, D. Shapira, J. McConnell, C. J. Gross, D. W. Stracener, H. Madani, E. Ch'avez, and M. E. Ortiz, Phys. Rev. C **60**, 021601 (1999).

[48] G. Nebbia, K. Hagel, D. Fabris, Z. Majka, J. B. Natowitz, R. P. Schmitt, B. Sterling, G. Mouchaty, G. Berkowitz, K. Strozewski, G. Viesti, P. I. Gonthier, B. Wilkins, M. N. Namboodiri, and H. Ho, Phys. Lett. B **176**, 20 (1986).

[49] K. Hagel, D. Fabris, P. Gonthier, H. Ho, Y. Lou, Z. Majka, G. Mouchaty, M. N. Namboodiri, J. B. Natowitz, G. Nebbia, R. P. Schmitt, G. Viesti, R. Wada, and B. Wilkins, Nucl. Phys. **A486**, 429 (1988).

[50] M. Gonin, L. Cooke, K. Hagel, Y. Lou, J. B. Natowitz, R. P. Schmitt, S. Shlomo, B. Srivastava, W. Turmel, H. Utsunomiya, R. Wada, G. Nardelli, G. Nebbia, G. Viesti, R. Zanon, B. Fornal, G. Prete, K. Niita, S. Hannuschke, P. Gonthier, and B. Wilkins, Phys. Rev. C **42**, 2125 (1990).

[51] A. Chbihi, L. G. Sobotka, N. G. Nicolis, D. G. Sarantites, D. W. Stracener, Z. Majka, D. C. Hensley, J. R. Beene, and M. L. Halbert, Phys. Rev. C **43**, 666 (1991).

[52] J. Gomez del Campo, D. Shapira, M. Korolija, H. J. Kim, K. Teh, J. Shea, J. P. Wieleczko, E. Ch'avez, M. E. Ortiz, A. Dacal, C. Volant, and A. D'Onofrio, Phys. Rev. C **53**, 222 (1996).

[53] D. Shapira, J. Gomez Del Campo, M. Korolija, J. Shea, C. F. Maguire, and E. Chavez-Lomeli, Phys. Rev. C **55**, 2448 (1997).

[54] C. B. Chitwood, D. J. Fields, C. K. Gelbke, D. R. Klesch, W. G. Lynch, M. B. Tsang, T. C. Awes, R. L. Ferguson, F. E. Obenshain, F. Plasil, R. L. Robinson, and G. R. Young, Phys. Rev. C **34**, 858 (1986).

[55] S. Shlomo and J. B. Natowitz, Phys. Rev. C **44**, 2878 (1991).

[56] A. L. Caraley, B. P. Henry, J. P. Lestone, and R. Vandenbosch, Phys. Rev. C **62**, 054612 (2000).

[57] J. Töke and W. J. Swiatecki, Nucl. Phys. **A372**, 141 (1981).

[58] F. Pühlhofer, Nucl. Phys. **A280**, 267 (1977).

[59] T. Ericson and V. Strutinski, Nucl. Phys. **8**, 284 (1958).

[60] T. Ericson, Adv. Phys. **9**, 425 (1960).

[61] D. Wilmore and P. E. Hodgson, Nucl. Phys. **55**, 673 (1964).

[62] C. M. Perey and F. G. Perey, At. Data Nucl. Data Tables **17**, 1 (1976).

[63] J. R. Huizenga and G. Igo, Nucl. Phys. **29**, 462 (1962).

[64] S. Cohen, F. Plasil, and W. J. Swiatecki, Ann. Phys. (N.Y.) **82**, 557 (1974).

[65] D. W. Lang, Nucl. Phys. **77**, 545 (1966).

[66] H. Vonach and M. Hille, Nucl. Phys. **A127**, 289 (1969).

[67] W. Dilg, W. Schantl, H. Vonach, and M. Uhl, Nucl. Phys. **A217**, 269 (1973).

[68] W. D. Myers and W. J. Swiatecki, Nucl. Phys. **81**, 1 (1966).

[69] B. Fornal, F. Gramegna, G. Prete, G. Nebbia, R. Smith, G.

D'Erasmo, L. Fiore, A. Pantaleo, G. Viesti, P. Blasi, F. Lucarelli, I. Iori, and A. Moroni, Phys. Rev. C **41**, 127 (1990).
[70] M. Kildir, G. La Rana, R. Moro, A. Brondi, A. D'Onofrio, E. Perillo, V. Roca, M. Romano, F. Terrasi, G. Nebbia, G. Viesti, and G. Prete, Phys. Rev. C **46**, 2264 (1992).
[71] N. G. Nicolis, D. G. Sarantites, L. G. Sobotka, and R. J. Charity, Phys. Rev. C **45**, 2393 (1992).
[72] W. D. Myers and W. J. Swiatecki, Ann. Phys. (N.Y.) **84**, 186 (1974).
[73] G. Viesti, V. Rizzi, D. Fabris, M. Lunardon, G. Nebbia, M. Cinausero, E. Fioretto, G. Prete, A. Brondi, G. La Rana, R. Moro, E. Vardaci, M. Aiche, M. M. Aleonard, G. Barreau, D. Boivin, J. N. Scheurer, J. F. Chemin, K. Hagel, J. B. Natowitz, R. Wada, S. Courtin, F. Haas, N. Rowley, B. M. Nyako, J. Gal, and J. Molnar, Phys. Lett. B **521**, 165 (2001).
[74] J. M. Alexander, M. T. Magda, and S. Landowne, Phys. Rev. C **42**, 1092 (1990).
[75] Sl. Cavallaro and F. Lo Piano, Nucl. Phys. **A627**, 379 (1997).